

VIPeR: Visual Incremental Place Recognition with Adaptive Mining and Lifelong Learning

Yuhang Ming^{1*}, Minyang Xu^{1*}, Xingrui Yang², Weicai Ye³, Weihan Wang⁴, Yong Peng^{1§},
Weichen Dai¹ and Wanzeng Kong¹

Abstract—Visual place recognition (VPR) is an essential component of many autonomous and augmented/virtual reality systems. It enables the systems to robustly localize themselves in large-scale environments. Existing VPR methods demonstrate attractive performance at the cost of heavy pre-training and limited generalizability. When deployed in unseen environments, these methods exhibit significant performance drops. Targeting this issue, we present VIPeR, a novel approach for visual incremental place recognition with the ability to adapt to new environments while retaining the performance of previous environments. We first introduce an adaptive mining strategy that balances the performance within a single environment and the generalizability across multiple environments. Then, to prevent catastrophic forgetting in lifelong learning, we draw inspiration from human memory systems and design a novel memory bank for our VIPeR. Our memory bank contains a sensory memory, a working memory and a long-term memory, with the first two focusing on the current environment and the last one for all previously visited environments. Additionally, we propose a probabilistic knowledge distillation to explicitly safeguard the previously learned knowledge. We evaluate our proposed VIPeR on three large-scale datasets, namely Oxford Robotcar, Nordland, and TartanAir. For comparison, we first set a baseline performance with naive finetuning. Then, several more recent lifelong learning methods are compared. Our VIPeR achieves better performance in almost all aspects with the biggest improvement of 13.65% in average performance.

I. INTRODUCTION

Visual place recognition (VPR) aims to recognize a previously visited place by giving visual observations like images. It is a core component in simultaneous localization and mapping (SLAM) systems [1] to ensure the robust operation of autonomous agents and augmented/virtual reality (AR/VR) systems in large-scale environments. When solving the VPR task, most of the existing approaches [2], [3], [4] cast it as a retrieval task. The solution then typically involves a two-step process, with step one generating global descriptors from local features and step two matching the descriptors to the ones in a database of place-tagged descriptors.

*Equal contribution, §Corresponding author
¹School of Computer Science, Hangzhou Dianzi University and Key Laboratory of Brain Machine Collaborative Intelligence of Zhejiang Province, Hangzhou, 310018, China. {yuhang.ming, minyangxu, yongpeng, weichendai, kongwanzeng}@hdu.edu.edu
²High-speed Aerodynamics Institute, CARDC, Mianyang, 621000, China. xingruiy@gmail.com
³State Key Lab of CAD&CG, Zhejiang University, Hangzhou, 310058, China. weicaiye@zju.edu.cn
⁴Stevens Institute of Technology, Hoboken, NJ, USA, 07030, wangl103@stevens.edu

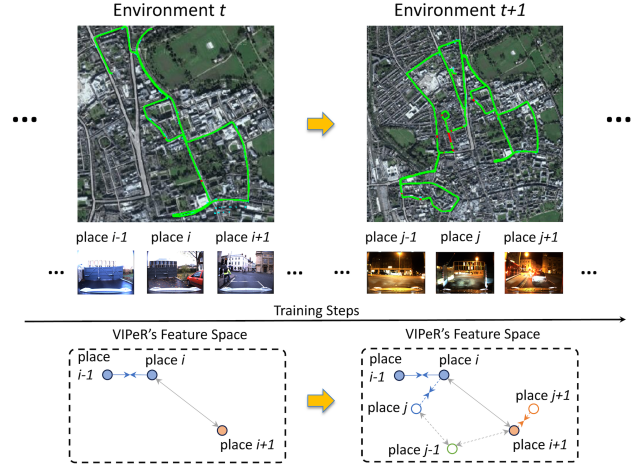


Fig. 1. Visual Incremental Place Recognition (VIPeR). Within a single environment, VIPeR aims to bring descriptors from the same place closer together and push those from different places farther apart in a learned feature space. When adapting to multiple environments, VIPeR is geared towards acquiring knowledge about new places while retaining information about previously encountered ones.

Traditionally, VPR methods use hand-craft local features or semantic features and construct global descriptors with vector of locally aggregated descriptors (VLAD) [5], graph-based descriptors [6], *etc.* More recently, following the success of NetVLAD [2], there have been notable advancements in end-to-end VPR methods in terms of accuracy [3], [4] and robustness [7], [8]. However, such a boost in performance comes at a cost. As the network architecture used in modern deep learning-based VPR methods getting much more complex, for example, KPConv [9] used in AEGIS-Net [4] and Transformer [10] used in R^2 Former [11], a laborious pre-training process that commonly takes days or even weeks becomes inevitable. In addition, because the trained models have a strong independent and identical distribution (i.i.d.) assumption on the test data, the performance drops considerably when the test data is collected from an unseen environment that doesn't follow the i.i.d. assumption.

However, when deploying the VPR-equipped autonomous agents and AR/VR systems in real-world scenarios, it is difficult to collect sufficient data that covers all potential environments beforehand to pre-train the deep learning-based models. Such a gap between the advance in deep learning-based VPR methods and the practical needs of autonomous agents and AR/VR systems leads to the fact that recent practical-oriented systems still prefer the traditional VPR methods [12], [13]. In this paper, we aim to close this gap by enabling the lifelong learning ability of the deep learning-

based VPR method. In particular, we present VIPeR, a visual incremental place recognition method that can adapt to the newly observed environment during deployment while reserving its knowledge of previously visited environments. Fig. 1 illustrates the core idea of the proposed VIPeR.

The idea of enabling lifelong learning for deep neural networks is not new. Also known as continual learning or incremental learning, it is designed to overcome the notorious catastrophic forgetting [14] when learning from sequential inputs. Despite that lifelong learning has been widely studied [15] and applied to many computer vision [16] or natural language processing [17] tasks, there is only a handful of works attempting to apply it to the place recognition task. AirLoop [18] and InCloud [19], as the pioneers in lifelong place recognition, both tackle the catastrophic forgetting with a simple memory structure and employ knowledge distillation [20] to constrain the training. AirLoop further employs the memory aware synapses (MAS) [21] for regularization.

Although achieving promising performance, there is still plenty of room for improvement. As pointed out in CCL [22], the naive triplet loss used in AirLoop [18] and InCloud [19] inevitably introduces bias when learning the global representation of various places. Such a phenomenon becomes even severe when hard-mining is applied to the training (see Table II). In addition, the naive choice of a simple memory structure substantially hinders the power of the rehearsal strategy. Finally, the deterministic knowledge distillation used in AirLoop and InCloud is very sensitive to the outliers in the data, leading to potential performance degradation.

Targeting these issues, we first introduce an adaptive mining scheme for triplet loss in metric learning. Our adaptive mining scheme can adaptively choose hard mining or soft mining, achieving a balanced performance between a single environment and multiple environments. Focusing on lifelong learning, we then draw inspiration from human memory systems and design a novel memory bank to store memories of multiple environments. Our memory bank is made of three components. For the current environment, we have a sensory memory bank and a working memory bank. For previously visited environments, we have another long-term memory bank. Finally, to make the model more robust against outliers, we extend the deterministic knowledge distillation used in AirLoop [18] and InCloud [19] to a probabilistic one. We conduct extensive experiments on three large-scale datasets and our proposed VIPeR demonstrates superior performance when compared to other state-of-the-art (SoTA) lifelong place recognition methods.

In summary, our contributions are as follows:

- We introduce an adaptive mining scheme for metric learning to balance the performance within a single environment and across multiple environments;
- We design a novel, brain-inspired memory bank for rehearsal, alleviating the effects of catastrophic forgetting;
- We propose a probabilistic knowledge distillation to regularize the training across different environments;
- We conduct extensive experiments on three publicly available datasets and demonstrate SoTA performance.

II. RELATED WORK

A. Lifelong Learning

Lifelong learning targets the sequential learning setting and focuses on improving the adaptability and generalizability of the deep learning models. However, naive solutions like finetuning on the new tasks make the model quickly forget the knowledge about previous tasks, resulting in catastrophic forgetting [14]. Addressing this issue, most existing methods can be categorized into rehearsal-based approaches and regularization-based approaches [16].

The core of the rehearsal-based approach is a memory buffer that either explicitly or implicitly stores samples from previous tasks. Then, when the model is trained on a new task, the samples stored in the buffer join the samples of the current task to refresh the model’s memory about previous tasks. Exemplary works in this approach are iCaRL [23], gradient episodic memory (GEM) [24], and deep generative replay (DGR) [25], which tackle the image classification task with iCaRL and GEM explicitly stores a small number of samples per class for rehearsal and DGR accompanies an additional generative model to enable implicit rehearsal.

Shifting the focus to the model itself, the regularization-based approach applies regularization on either the weight or the function. Regarding weight regularization, it commonly evaluates the importance of the model’s parameters on previous tasks and mitigates the performance degradation by introducing a penalty for the loss. Within this scope, elastic weight consolidation (EWC) [26] employs the Fisher information matrix to calculate the importance, while syntactic intelligence (SI) [27] and memory aware synapses (MAS) [21] both favor the online importance estimation. Then, in function regularization, various knowledge distillation approaches have been explored to distill the knowledge of old models to the new ones. An example work is learning without forgetting (LwF) [28], which performs distillation by comparing the predictions from the output head of the old tasks to the ones of new tasks.

B. Learning-based Place Recognition

NetVLAD [2], as a milestone work in the learning-based VPR method, modified the VLAD [5] descriptor to make it differentiable and enabled end-to-end training of VPR methods. Demonstrating the representation power of the deep learning models, it inspires a plethora of works to promote the performance of deep learning-based VPR methods.

To improve the performance with image inputs, SPE-VLAD [29] explored the spatial pyramid structure of images to make the VLAD descriptor aware of structural information. Addressing the problems of appearance and viewpoint changes, Patch-NetVLAD [30] proposed to combine the advantages of local and global features by fusing multi-scale patch-level features that are computed from NetVLAD residuals. Moving on to 3D inputs like point clouds, Point-NetVLAD [31] is a straightforward extension of NetVLAD by replacing the 2D CNN with the PointNet [32] model to handle the input point clouds of fixed sizes. To empower the

model to deal with inputs of random sizes, FusionVLAD [7] and AEGIS-Net [4] adopted more advanced 3D CNN with FusionVLAD focusing on cross-viewpoint VPR and AEGIS-Net concentrating on aggregating multi-level features.

On the other hand, despite the fact that NetVLAD [2] is one of the most popular global descriptors, other global descriptors have also been explored. To start with, various forms of pooling have been employed for global descriptor generation due to their simplicity and generalizability. For example, APANet [33] favors sum pooling, Gordo *et al.* [34] chooses max pooling R-MAC [35], MinkLoc3D [36] adopts generalized-mean pooling (GeM) [37]. More recently, with Transformer [10] prevailing in a wide range of tasks, it has also been used to create global descriptors in VPR. For example, R^2 Former [11] employs attention weights to guide the aggregations of local tokens.

Although tremendous advances have been witnessed in VPR research, most of the work tackles the task under the batch learning setting with the complete dataset available prior to the training. However, our paper investigates the VPR task under a sequential learning setting, which is addressed by a few works.

More related to our work, BioSLAM [38] tackles the VPR task from a lifelong learning perspective and chooses the generative replay from a rehearsal-based approach with a dual memory zone to store the previous observations. Nevertheless, AirLoop [18] combines a rehearsal-based approach with a regularization-based approach to mitigate the catastrophic forgetting issue with a lightweight model. Following this idea, InCloud [19] and CCL [22] extend to point cloud input with InCloud introducing an angular-based knowledge distillation to relax the function regularization and CCL favoring contrast learning with InfoNCE [39] loss over metric learning with triplet loss [40]. Although we also build our work on AirLoop, our proposed VIPeR significantly differs from the above-mentioned methods with the adaptive mining for metric learning with triplet loss, a delicately designed three-zone memory bank for rehearsal, and probabilistic knowledge distillation (PKD) for regularization.

III. METHOD

As with many previous works on VPR, we cast the task of visual incremental place recognition as a retrieval problem. In particular, we define a sequence of environments $\mathcal{E} = \{E_0, E_1, \dots, E_t, \dots\}$ with only one environment being available for training at a time. Furthermore, we define a set of images as observations for each environment $E_t = \{I_0, I_1, \dots, I_i, \dots\}$, which is also acquired in a sequential manner. Then, the VPR task is solved by incrementally constructing a database of place-tagged global descriptors $\mathcal{G} = \{\mathbf{g}_0, \dots, \mathbf{g}_i, \dots\}$ with each one generated with $\mathbf{g}_i = f(I_i)$. $f(\cdot)$ here is a trainable model that consists of two sub-models, one extracts local features from input images and the other one aggregates the local features into global descriptors. Whenever the query image I_q becomes available, the same model is used to generate a global descriptor from the query image $\mathbf{d}_q = f(I_q)$. Following this, by matching the query descriptor to

the database descriptors, we can retrieve the top- K closest neighbors of the query image as the recognized places. In the following, we present VIPeR to tackle visual incremental place recognition by combining metric learning with lifelong learning. An overview of VIPeR is shown in Fig. 2.

A. Metric Learning

To train our model, we adopt metric learning with triplet loss. We first construct input triplet \mathcal{T} with an anchor image I^{anc} that represents a place in the environment, m positive images $I^{pos} = \{I_0^{pos}, I_1^{pos}, \dots, I_m^{pos}\}$ that are taken from the same place, and n negative images $I^{neg} = \{I_0^{neg}, I_1^{neg}, \dots, I_n^{neg}\}$ that are taken from different places. Then, given the triplet $\mathcal{T} = (I^{anc}, I^{pos}, I^{neg})$, we drew inspiration from the naive triplet loss [40] and hard triplet loss [41], and introduced adaptive triplet loss to train our model.

The naive triplet loss [40] is defined as

$$L_{triplet} = \max(s_j^{an} - s_i^{ap} + \delta, 0), \quad (1)$$

where $s_j^{an} = \text{sim}(f(I^{anc}), f(I_j^{neg}))$ is the cosine similarity between the global descriptors generated from the anchor image and a negative image sample, s_i^{ap} is the cosine similarity between the ones from the anchor and a positive image sample, δ is a hyper-parameter indicating the margin. When selecting the positive and negative image, the naive triplet loss opted for a random mining strategy with the sample indices i and j randomly selected. Despite that, the naive triplet loss exhibits better generalizability and is used in previous works like AirLoop [18] and InCloud [19]; it also makes the training process less effective, resulting in less discriminative global descriptors.

The hard triplet loss [41], to the contrary, goes to another extreme and favors the hard mining strategy. When choosing the sample images, the hard triplet loss focuses on the most difficult sample with the sample indices selected as $i = \text{argmin}_i(s_i^{ap})$ and $j = \text{argmax}_j(s_j^{an})$. Such a strategy largely increases the discrimination of the global descriptor and has been widely used by PointNetVLAD [31], AEGIS-Net [4] for place recognition in a single large-scale environment. However, such a mining strategy inevitably introduces bias into the training, leading to performance degradation in life-long learning settings. We later demonstrate this in Table III in the ablation study.

To best join the advantages of random mining and hard mining, we propose a novel adaptive mining strategy and adjust the difficulty level of the training samples based on the fluctuations of the loss. We denote the triplet loss under the adaptive mining strategy as $L_{ada-triplet}$. Specifically, we keep tracking the changes in the loss during the training process. In the case when the loss increases in the current training step with the increment larger than a hyper-parameter T_d , we say the chosen training sample is too difficult, and we incline to a simpler sample in the following training steps. Contrarily, if the loss decreases in the current step with a decrement bigger than another hyper-parameter T_e , we determine the current training sample is too easy, and we lean towards more difficult ones. Under such a mining design, we

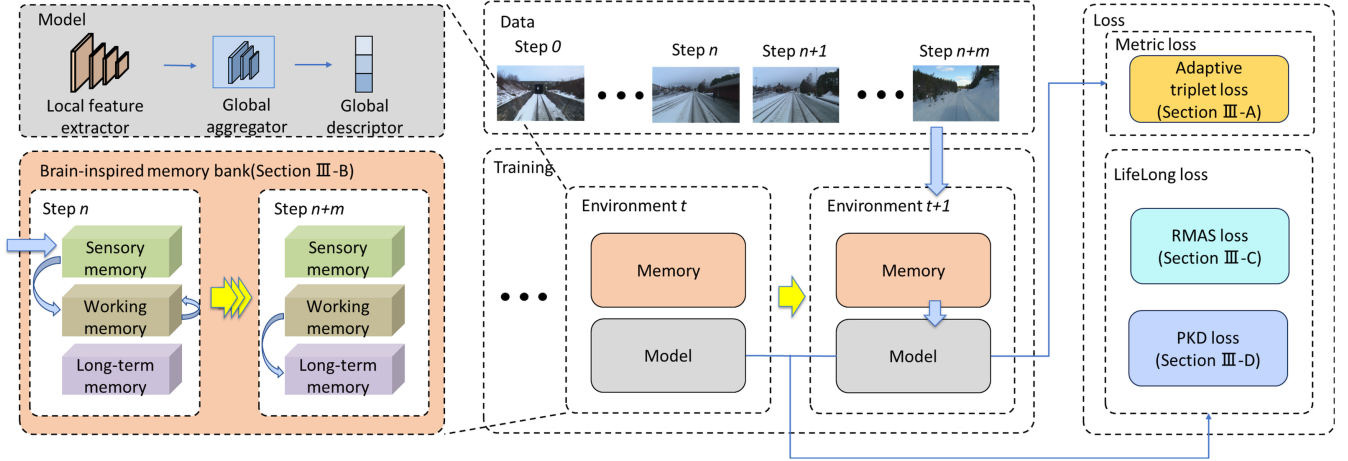


Fig. 2. Overview of main components and data flow within our proposed VIPeR. To alleviate the catastrophic forgetting in lifelong learning, our proposed VIPeR accompanies the place recognition model with a brain-inspired memory bank for rehearsal, and adaptive mining, relational memory aware synapses (RMAS) and probabilistic knowledge distillation (PKD) for regularization. achieve a balance between the discrimination requirements for place recognition and the generalizability requirements for handling the sequential input.

B. Brain-inspired Memory Bank

To alleviate the notorious catastrophic forgetting in life-long learning, we first investigate the rehearsal-based approach to refresh the model’s memory about previous environments. Specifically, we present a brain-inspired memory bank $\mathcal{B} = (M, R)$ with a fixed-size image storage space M and a corresponding adjacency matrix R . Each element in the adjacency matrix $R_{i,j}$ represents the relative location between place i and place j , which is then used to determine whether these two places belong to a positive or a negative pair.

Regarding the fixed-size image storage space M , we mimic the human memory system and design the architecture as a composition of a per-environment sensory memory M^{sn} , a per-environment working memory M^{wk} , and an environment-agnostic long-term memory M^{lt} . Our brain-inspired memory bank is capable of improving the model’s adaptability in a new environment while preserving its stability over all previous environments. We illustrate the update process of the proposed brain-inspired memory bank in Fig. 2.

For any unseen environment t , the sensory memory M_t^{sn} , which is a first-in-first-out queue of size l^{sn} , is always first activated and used to store the most recently visited places. With such a design, we ensure the model stays sensitive to the latest changes in the scene. Whenever the sensory memory is full, the working memory M_t^{wk} , as a list of size l^{wk} , is activated to store the places coming out of the sensory memory. When the working memory is also full, we decide on whether the new place should be stored with a probability $p = l^{wk}/num$, where num is the total number of images that have passed in the current environment. This makes the working memory a perfect complement to the sensory memory since the probability of updating the working memory keeps decreasing as more images are processed, allowing the old observations to be preserved.

The long-term memory M^{lt} , also as a list of size l^{lt} ,

stores the samples of places from all previously visited environments to ensure its environment-agnostic property. When entering a new environment t , the long-term memory M_t^{lt} is updated following

$$M_t^{lt} = \omega M_{t-1}^{wk} + (1 - \omega) M_{t-1}^{lt}, \quad (2)$$

where M_{t-1}^{wk} and M_{t-1}^{lt} are the working memory and the long-term of environment $t - 1$, ω is a hyper-parameter to control the update ratio.

C. Relational Memory Aware Synapses

Additionally, we explore a weight regularization approach to prevent undesired weight updates when the model is adapting to the new environment. Particularly, we follow the relational memory aware synapses (RMAS) proposed in AirLoop [18] to estimate the importance weight Ω_t^{RMAS} of each parameter θ in the environment t . Then, the changes in the parameters are penalized with a regularization loss L_{RMAS} . Note that for simplicity, we omit the subscript t to index the environment in the loss function. We hereby briefly review the formulation of RMAS. For more details, we refer the readers to the original AirLoop [18] paper.

For environment t , the weight is approximated as

$$\Omega_t^{RMAS} \approx \frac{1}{N_t} \sum_{k=1}^{N_t} \left(\frac{\partial \|\tilde{S}_{k,t}\|_F}{\partial \theta} \right)^2, \quad (3)$$

where N_t is the number of images that have been processed, $\|\cdot\|_F$ is the Frobenius norm, $\tilde{S}_{k,t} \in \mathbb{R}^{3 \times 3}$ is the Gram matrix at the k -th training step. Each element in the Gram matrix is computed using the triplets we selected with adaptive mining in Section III-A, following $\tilde{S}_{k,t|(0,0)} = s^{aa}$, $\tilde{S}_{k,t|(0,1)} = s_i^{ap}$, $\tilde{S}_{k,t|(0,2)} = s_j^{an}$, etc..

Then, the RMAS loss is computed as

$$L_{RMAS} = \sum_{\theta \in \Theta} \Omega_{t-1}^{RMAS} (\theta_t - \theta_{t-1})^2, \quad (4)$$

where Θ is the set of all parameters, θ_t and θ_{t-1} indicate the updated parameter in the current environment t and the frozen parameter after training on environments $1, 2, \dots, t - 1$.

D. Probabilistic Knowledge Distillation

Moreover, we delve into the function regularization approach with knowledge distillation to further enhance the model’s adaptability to unseen environments during lifelong learning. Although previous works like AirLoop [18] and InCloud [19] have also explored knowledge distillation, we believe that their performance is limited due to two reasons. First of all, when selecting memory samples for distillation, these works use images from the current environment. We claim that such a choice is counter-intuitive as the previous model hasn’t seen the current environment, and its performance cannot be guaranteed. Secondly, these works opt for deterministic distillation with angular metrics, which makes the model more focused on local structures of samples.

To select more effective samples, we propose to only use the samples from the long-term memory M^l of our brain-inspired memory bank to perform knowledge distillation. Besides, we present PKD to make the model pay more attention to the global distribution of the samples. To estimate the distribution of the samples in the learned feature space, we first construct the matrices H_t and H_{t-1} using the model trained in the current environment t and the frozen model that has been trained on environment $1, 2, \dots, t-1$ respectively. Specifically, elements in the matrix are computed as

$$H_{\Xi|i,j} = \frac{\mathbf{g}_{i,\Xi} \cdot \mathbf{g}_{j,\Xi}}{\sqrt{d}} \quad \text{for } \Xi \in [t-1, t], \quad (5)$$

where d is the dimension of the global descriptor \mathbf{g} . Although similar ideas can be seen in CCL [22], we notice that their design with the distillation temperature hyper-parameter easily leads to a vanishing gradient during the training process. We are inspired by Transformer [10] and make a simple yet effective modification by replacing the distillation temperature hyper-parameter with a model-specific value \sqrt{d} to prevent the gradients vanishing issues.

Once the H matrices are computed, we can estimate the distribution with the softmax (SM) function and calculate the PKD loss with Kullback-Leibler (KL) divergence as

$$L_{PKD} = \sum_{i,j} KL \{ \text{SM}(H_{t-1|i,j}) \log(\text{SM}(H_{t|i,j})) \}. \quad (6)$$

E. Final Loss

Finally, we combine the above-mentioned loss functions into the final loss function of the following form

$$L = L_{ada-triplet} + \lambda_1 L_{RMAS} + \lambda_2 L_{PKD}, \quad (7)$$

where λ_1 and λ_2 are hyper-parameters used to adjust the contributions of the RMAS and PKD loss functions.

IV. EXPERIMENT

A. Implementation Details

When choosing the VPR method, we first experiment with the same VPR method used in AirLoop [18], which consists of a pre-trained VGG-19 [42] for local feature extraction and GeM [37] for global descriptor aggregation. The hyper-parameter in GeM also follows AirLoop as $p = 3$, and the dimension of its global descriptor is set to $d = 1024$. Additionally, to get more discriminative global descriptors,

we extend the VPR method by replacing the GeM layer with a NetVLAD layer [2]. We especially follow many other VPR methods like [2], [31], [3], [4] and set the number of clusters to $K = 64$. However, we set the dimension of global descriptors generated by NetVLAD to be the same as that of GeM descriptors.

When forming the triplet tuple, we empirically set the number of positive and negative samples to be $m = 1$ and $n = 5$. And we set the margin in Eq. 1 to be $\delta = 1$. Regarding adaptive mining, we prevent the model from always learning with easy samples by explicitly setting the threshold for using easier samples to be higher than the one for using more difficult ones. Especially, we choose $T_d = 0.02$ and $T_e = 0.01$.

As for the brain-inspired memory bank, we ensure a fair comparison by setting the total size of our memory bank to be the same as the queue’s length in AirLoop [18]. Particularly, we empirically divide the total size into $l^s = 500$ for sensory memory, $l^{wk} = 400$ for working memory, and $l^l = 100$ for long-term memory. In addition, we set the hyper-parameter in Eq. 2 to be $\omega = 0.5$.

Finally, for Eq. 7, we choose equal weights with hyper-parameters $\lambda_1 = 1$ and $\lambda_2 = 1$. We train the VPR methods using the stochastic gradient descent (SGD) optimizer with a learning rate of 0.002 and a momentum of 0.9.

B. Datasets and Evaluation Metrics

Datasets: We evaluate our proposed VIPeR on three large-scale, publicly available datasets, namely Oxford RobotCar [43], Nordland [44], and TartanAir [45].

Oxford RobotCar [43] is a real-world autonomous driving dataset with data collected under various weather conditions across multiple urban environments in Oxford. For evaluation, we follow AirLoop [18] and select three environments under the tag “sun”, “overcast”, and “night”. For each environment, the same two sequences are selected for training and testing. We define two images belonging to the same place if the distance between them is less than 10m and the yaw difference is less than 15° .

Nordland [44] is also a real-world dataset with across-season data collected from a railway journey through the Nordland region of Norway. As AirLoop [18], we also use the recommended train-test split and determine whether two images are taken from the same place if they are separated by three images or less.

TartanAir [45] is a photo-realistic synthetic dataset. It covers both indoor and outdoor environments and provides data collected under diverse lighting conditions, weather conditions, and times of the day. Also following AirLoop [18], we select 5 environments for evaluation with the same surface intersection-over-union (sIoU) used as the criteria to decide whether two images are from the same place. Specifically, we set $sIoU < 0.1$ for negative, $sIoU > 0.7$, and $sIoU > 0.5$ for positive in training and test, respectively.

Evaluation metrics: In line with AirLoop [18], we use the recall rate at 100% precision as the core metric to evaluate the model’s performance on single environments. To better assess the performance in lifelong learning, we evaluate the

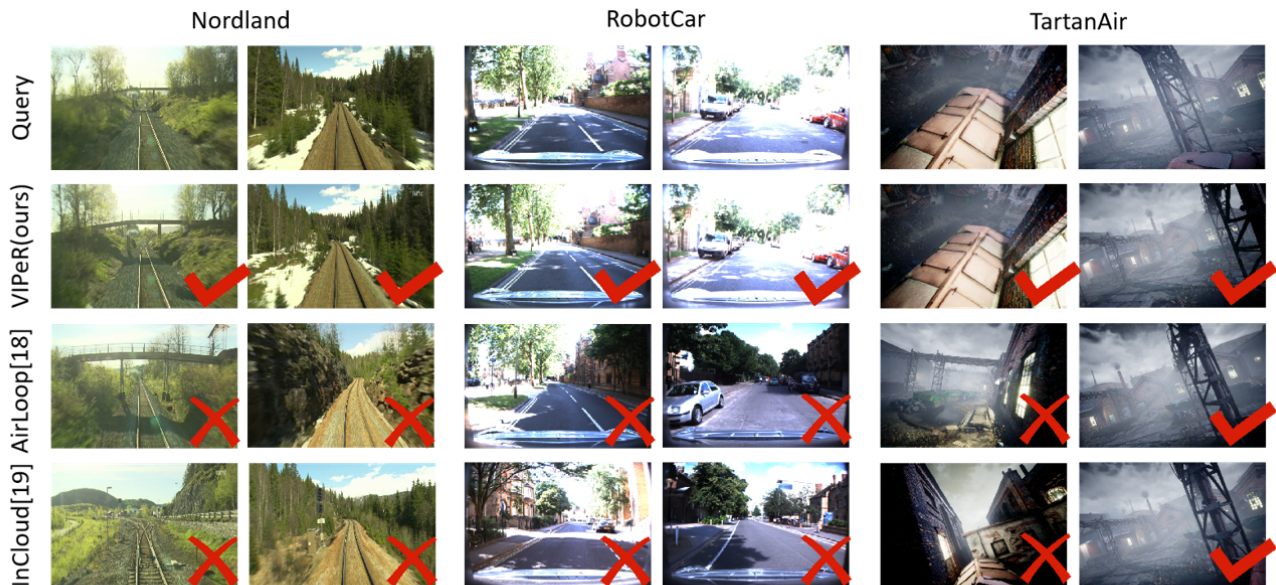


Fig. 3. Top-1 retrieval of the model trained for T environments and evaluated on the first environment. Our VIPeR can better discriminate similar places and exhibits better resilience to catastrophic forgetting.

model trained after each environment on every environment in the environment sequence \mathcal{E} of length T , even the unseen ones. We summarize the results in an evaluation matrix $P \in \mathbb{R}^{T \times T}$ with each of its element $P_{i,j}$ being the recall rate at 100% precision when evaluating the model trained after environment i in environment j .

Given the evaluation matrix, we further compute the average performance (AP), backward transfer (BWT), and forward transfer (FWT), which are introduced in [24], to evaluate the overall performance, how does learning in new environments affect the previous knowledge, and how well does the model generalize to unseen environments. We refer readers to [24] for the detailed formulas for computation.

C. Evaluation and Discussions

For comparison, we first set a baseline performance with naive finetuning on both of the VPR methods we experimented with. In addition, we also explore the performance of two generic weight regularization methods in lifelong learning, EWC [26] and SI [27]. For more recent methods, we compare our proposed VIPeR to AirLoop [18] and InCloud [19], which are specifically designed for visual incremental place recognition. However, because AirLoop only provided the performance with the combination of VGG-19 [42] and GeM [37], we re-train AirLoop with their official implementation to get its performance with the combination of VGG-19 and NetVLAD [2]. Similarly, since InCloud was only tested with LiDAR point clouds, we replaced its VPR methods with the same one that our VIPeR experimented with and re-trained the InCloud model with their official implementation.

We present the qualitative results in Fig. 3 with VIPeR, AirLoop [18], and InCloud [19] trained for all available environments and evaluated on the very first one to demonstrate the model’s resilience to catastrophic forgetting. Then, we also present quantitative results in all three environments

in Table I. It can be seen that naive finetuning and generic weight regularization method EWC [26] and SI [27] exhibit inferior performance, especially in AP and BWT, indicating their inadequate abilities when fighting against catastrophic forgetting in visual incremental place recognition. Furthermore, despite that both AirLoop [18] and InCloud [19] achieved improved performance over baseline methods by utilizing a combination of several lifelong learning methods to mitigate the catastrophic forgetting, they suffer from a notable performance drop when changing from GeM [37] to more discriminative NetVLAD [2].

The results of our proposed VIPeR exhibit superior performance over other methods in almost all metrics. In particular, our VIPeR prevails in terms of AP and FWT across all three datasets, which implies the model’s strong performance and good generalizability towards unseen environments. In terms of BWT, which measures the forgetfulness of the model, our VIPeR didn’t to achieve the best performance. However, we argue this amount forgetting is acceptable as even after forgetting some knowledge of the previous visited place, our VIPeR still exhibits better recognition performance when compared to AirLoop and InCloud. Additionally, when changing the global descriptor aggregator from GeM to NetVLAD, our VIPeR, unlike AirLoop [18] or InCloud [19], achieves even better performance, which further demonstrates the effectiveness of presented solutions.

D. Ablation Study

We further investigate the contribution of the adaptive mining, brain-inspired memory bank, and PKD loss by replacing the corresponding modules in the base model, *i.e.* AirLoop [18], one at a time.

Adaptive Mining: To start with, we replace the random mining with hard mining, which is commonly used in VPR tasks, and the proposed adaptive mining. We conduct experiments in all three datasets as above and present the

TABLE I

PERFORMANCE COMPARISON OF LIFELONG PLACE RECOGNITION METHODS. ALL THE RESULTS ARE OBTAINED WITH VGG-19 [42] AND THE ONES MARKED WITH § ARE DIRECTLY TAKEN FROM AIRLOOP [18]. **BOLDFACE** AND UNDERLINE INDICATE THE BEST AND SECOND-BEST RESULTS.

Feature Aggregator	Method	Oxford RobotCar			Nordland			TartanAir		
		AP \uparrow	BWT \uparrow	FWT \uparrow	AP \uparrow	BWT \uparrow	FWT \uparrow	AP \uparrow	BWT \uparrow	FWT \uparrow
GeM [37]	§Finetune	0.411	-0.066	0.462	0.615	-0.012	0.549	0.754	-0.009	0.730
	§EWC [26]	0.416	-0.054	0.461	0.614	-0.014	0.549	0.758	-0.005	0.728
	§SI [27]	0.407	-0.062	0.454	0.614	-0.010	0.549	0.753	-0.010	0.730
	§AirLoop [18]	0.461	-0.013	0.485	0.631	<u>0.018</u>	0.546	0.769	0.007	0.736
	AirLoop [18]	0.454	-0.028	0.481	0.622	0.009	0.553	0.776	0.009	0.753
	InCloud [19]	<u>0.491</u>	-0.003	<u>0.507</u>	0.624	0.017	0.532	0.776	<u>0.018</u>	0.749
	VIPeR(ours)	0.477	0.002	0.485	<u>0.661</u>	-0.002	0.620	0.738	0.004	0.721
NetVLAD [2]	Finetune	0.379	-0.068	0.413	0.641	-0.006	0.543	0.770	0.009	0.759
	AirLoop [18]	0.416	-0.065	0.501	0.639	-0.001	0.549	0.782	0.021	0.756
	InCloud [19]	0.445	0.050	0.413	0.622	0.039	0.505	0.771	<u>0.018</u>	0.754
	VIPeR(ours)	0.558	0.034	0.540	0.670	-0.009	<u>0.587</u>	0.787	0.007	0.772

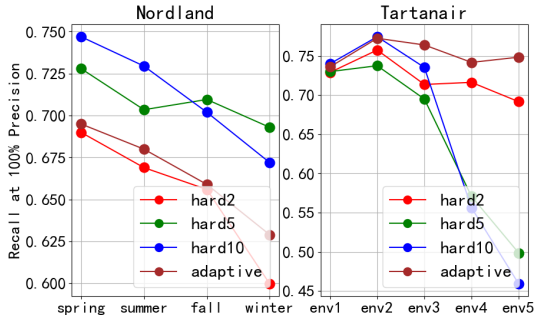


Fig. 4. Performance of different mining strategies on Nordland and TartanAir datasets. “hard2”, “hard5”, “hard10” indicate the performance of using the hard mining strategy with 2, 5, and 10 negative samples.

TABLE II

COMPARISON OF DIFFERENT DATA MINING STRATEGIES ON THE OXFORD ROBOTCAR DATASET

Method	AP \uparrow	BWT \uparrow	FWT \uparrow
random mining	0.454	-0.028	0.481
2 hard mining	0.267	-0.115	0.371
5 hard mining	0.112	-0.010	0.096
10 hard mining	0.161	-0.027	0.161
adaptive mining	0.559	-0.020	0.587

results in Fig. 4 and Table II. The adaptive mining strategy used in our proposed VIPeR exhibits favorable performances in TartanAir [45] and Oxford RobotCar [43], outperforming random mining used in the base model and hard mining used in VPR methods with batched inputs. Although our adaptive mining does not perform as good as hard mining in Nordland [44] when we increasing the number of negative samples, we believe it is mainly caused by the repetitive scenes between different environments in Nordland. We argue that hard mining introduces serious bias into the learning process, which is demonstrated by the drastic performance drop in TartanAir and Oxford RobotCar.

Brain-inspired Memory Bank: Then, we replace the naive queue used in the base model with the brain-inspired memory bank in the proposed VIPeR and present the quantitative results on Oxford RobotCar [43] dataset in Table III. It is notable that the brain-inspired memory bank surpasses the naive queue with a large margin across all evaluation metrics. The results demonstrate the superior performance of the brain-inspired memory bank in lifelong learning with good generalizability and resilience to catastrophic forgetting.

TABLE III

COMPARISON OF DIFFERENT REHEARSAL METHODS ON THE OXFORD

ROBOTCAR DATASET			
Method	AP \uparrow	BWT \uparrow	FWT \uparrow
naive queue	0.454	-0.028	0.481
memory bank	0.494	0.016	0.510

TABLE IV

COMPARISON OF DIFFERENT KNOWLEDGE DISTILLATION METHODS ON

THE OXFORD ROBOTCAR DATASET

Method	AP \uparrow	BWT \uparrow	FWT \uparrow
Finetune	0.411	-0.066	0.462
RKD	0.454	-0.028	0.481
AKD	0.491	-0.003	0.507
PKD	0.558	0.005	0.567

Probabilistic Knowledge Distillation: Finally, replace the relational knowledge distillation in the base model with the PKD used in the proposed VIPeR. In addition, we also compare with performance of angular-based knowledge distillation proposed in InCloud [19]. As shown in Table IV, it is evident that our probabilistic distillation largely exceeds the performance of relational knowledge distillation and angular-based knowledge distillation, let alone the naive finetuning strategy. The extraordinary results validate that our distillation approach is capable of grasping the underlying data distribution, which is a big advantage in dealing with catastrophic forgetting and the adaptability when training in unseen environments.

V. CONCLUSIONS

In this work, we propose VIPeR, a visual incremental place recognition method. We investigate triplet mining strategies suitable for lifelong learning and find a balance between per-environment and cross-environment performance with the proposed adaptive mining. In addition, we mitigate the catastrophic forgetting issues by combining a rehearsal-based approach with a regularization-based approach. In particular, we design a novel brain-inspired memory bank to mimic the human memory system and present a probabilistic knowledge distillation. We conduct extensive experiments on large-scale datasets, the results of which demonstrate the effectiveness of the proposed VIPeR. As for future work, we believe there are many possible directions, like extending the VIPeR model to handle other forms of single-modality input or cross-modality input.

REFERENCES

- [1] X. Yang, Y. Ming, Z. Cui, and A. Calway, "FD-SLAM: 3-d reconstruction using features and dense matching," in *International Conference on Robotics and Automation*, 2022.
- [2] R. Arandjelovic, P. Gronat, A. Torii, T. Pajdla, and J. Sivic, "Netvlad: Cnn architecture for weakly supervised place recognition," in *IEEE Conference on Computer Vision and Pattern Recognition*, 2016.
- [3] Y. Ming, X. Yang, G. Zhang, and A. Calway, "CGiS-net: Aggregating colour, geometry and implicit semantic features for indoor place recognition," in *IEEE/RSJ International Conference on Intelligent Robots and Systems*, 2022.
- [4] Y. Ming, J. Ma, X. Yang, W. Dai, Y. Peng, and W. Kong, "AEGIS-Net: Attention-guided multi-level feature aggregation for indoor place recognition," in *IEEE International Conference on Acoustics, Speech and Signal Processing*, 2024.
- [5] H. Jégou, M. Douze, C. Schmid, and P. Pérez, "Aggregating local descriptors into a compact image representation," in *IEEE Computer Society Conference on Computer Vision and Pattern Recognition*, 2010.
- [6] Y. Ming, X. Yang, and A. Calway, "Object-augmented rgb-d slam for wide-disparity relocalisation," in *IEEE/RSJ International Conference on Intelligent Robots and Systems*, 2021.
- [7] P. Yin, L. Xu, J. Zhang, and H. Choset, "Fusionvlad: A multi-view deep fusion networks for viewpoint-free 3d place recognition," *IEEE Robotics and Automation Letters*, vol. 6, no. 2, 2021.
- [8] P.-Y. Lajoie and G. Beltrame, "Self-supervised domain calibration and uncertainty estimation for place recognition," *IEEE Robotics and Automation Letters*, vol. 8, no. 2, 2023.
- [9] H. Thomas, C. R. Qi, J.-E. Deschaud, B. Marcotegui, F. Goulette, and L. Guibas, "Kpconv: Flexible and deformable convolution for point clouds," in *IEEE/CVF International Conference on Computer Vision*, 2019.
- [10] A. Vaswani, N. Shazeer, N. Parmar, J. Uszkoreit, L. Jones, A. N. Gomez, L. Kaiser, and I. Polosukhin, "Attention is all you need," in *International Conference on Neural Information Processing Systems*, 2017.
- [11] S. Zhu, L. Yang, C. Chen, M. Shah, X. Shen, and H. Wang, "R² former: Unified retrieval and reranking transformer for place recognition," in *IEEE/CVF Conference on Computer Vision and Pattern Recognition*, 2023.
- [12] P. Vial, N. Palomeras, J. Solà, and M. Carreras, "Underwater pose slam using gmm scan matching for a mechanical profiling sonar," *Journal of Field Robotics*, vol. 41, no. 3, 2024.
- [13] X. Yi, Y. Zhou, M. Habermann, V. Golyanik, S. Pan, C. Theobalt, and F. Xu, "Egolocate: Real-time motion capture, localization, and mapping with sparse body-mounted sensors," *ACM Trans. Graph.*, vol. 42, jul 2023.
- [14] B. Pfülb and A. Gepperth, "A comprehensive, application-oriented study of catastrophic forgetting in dnns," in *International Conference on Learning Representations*, 2019.
- [15] L. Wang, X. Zhang, H. Su, and J. Zhu, "A comprehensive survey of continual learning: Theory, method and application," *IEEE Transactions on Pattern Analysis and Machine Intelligence*, 2024.
- [16] M. De Lange, R. Aljundi, M. Masana, S. Parisot, X. Jia, A. Leonardis, G. Slabaugh, and T. Tuytelaars, "A continual learning survey: Defying forgetting in classification tasks," *IEEE Transactions on Pattern Analysis and Machine Intelligence*, vol. 44, no. 7, 2022.
- [17] M. Biesialska, K. Biesialska, and M. Costa-jussà, "Continual lifelong learning in natural language processing: A survey," in *International Conference on Computational Linguistics*, 2020.
- [18] D. Gao, C. Wang, and S. Scherer, "Airloop: Lifelong loop closure detection," in *International Conference on Robotics and Automation*, 2022.
- [19] J. Knights, P. Moghadam, M. Ramezani, S. Sridharan, and C. Fookes, "Incloud: Incremental learning for point cloud place recognition," in *IEEE/RSJ International Conference on Intelligent Robots and Systems*, 2022.
- [20] S. Hou, X. Pan, C. C. Loy, Z. Wang, and D. Lin, "Lifelong learning via progressive distillation and retrospection," in *European Conference on Computer Vision*, 2018.
- [21] R. Aljundi, F. Babiloni, M. Elhoseiny, M. Rohrbach, and T. Tuytelaars, "Memory aware synapses: Learning what (not) to forget," in *European Conference on Computer Vision*, 2018.
- [22] J. Cui and X. Chen, "Ccl: Continual contrastive learning for lidar place recognition," *IEEE Robotics and Automation Letters*, vol. 8, no. 8, 2023.
- [23] S.-A. Rebuffi, A. Kolesnikov, G. Sperl, and C. H. Lampert, "icarl: Incremental classifier and representation learning," in *IEEE Conference on Computer Vision and Pattern Recognition*, 2017.
- [24] D. Lopez-Paz and M. Ranzato, "Gradient episodic memory for continual learning," in *International Conference on Neural Information Processing Systems*, 2017.
- [25] H. Shin, J. K. Lee, J. Kim, and J. Kim, "Continual learning with deep generative replay," in *International Conference on Neural Information Processing Systems*, 2017.
- [26] J. Kirkpatrick, R. Pascanu, N. Rabinowitz, J. Veness, G. Desjardins, A. Rusu, K. Milan, J. Quan, T. Ramalho, A. Grabska-Barwinska, D. Hassabis, C. Clopath, D. Kumaran, and R. Hadsell, "Overcoming catastrophic forgetting in neural networks," *Proceedings of the National Academy of Sciences*, vol. 114, 3 2017.
- [27] F. Zenke, W. Gerstner, and S. Ganguli, "The temporal paradox of hebbian learning and homeostatic plasticity," *Current Opinion in Neurobiology*, vol. 43, 2017.
- [28] Z. Li and D. Hoiem, "Learning without forgetting," *IEEE Transactions on Pattern Analysis and Machine Intelligence*, vol. 40, no. 12, 2017.
- [29] J. Yu, C. Zhu, J. Zhang, Q. Huang, and D. Tao, "Spatial pyramid-enhanced netvlad with weighted triplet loss for place recognition," *IEEE Transactions on Neural Networks and Learning Systems*, vol. 31, no. 2, 2020.
- [30] S. Hausler, S. Garg, M. Xu, M. Milford, and T. Fischer, "Patch-netvlad: Multi-scale fusion of locally-global descriptors for place recognition," in *IEEE/CVF Conference on Computer Vision and Pattern Recognition*, 2021.
- [31] M. A. Uy and G. H. Lee, "Pointnetvlad: Deep point cloud based retrieval for large-scale place recognition," in *IEEE/CVF Conference on Computer Vision and Pattern Recognition*, 2018.
- [32] R. Q. Charles, H. Su, M. Kaichun, and L. J. Guibas, "Pointnet: Deep learning on point sets for 3d classification and segmentation," in *IEEE Conference on Computer Vision and Pattern Recognition*, 2017.
- [33] Y. Zhu, J. Wang, L. Xie, and L. Zheng, "Attention-based pyramid aggregation network for visual place recognition," in *ACM International Conference on Multimedia*, 2018.
- [34] A. Gordo, J. Almazán, J. Revaud, and D. Larlus, "End-to-end learning of deep visual representations for image retrieval," *International Journal of Computer Vision*, vol. 124, 6 2017.
- [35] G. Toliás, R. Sivic, and H. Jégou, "Particular object retrieval with integral max-pooling of CNN activations," in *International Conference on Learning Representations*, 2016.
- [36] J. Komorowski, "Minkloc3d: Point cloud based large-scale place recognition," in *IEEE Winter Conference on Applications of Computer Vision (WACV)*, 2021.
- [37] F. Radenović, G. Toliás, and O. Chum, "Fine-tuning cnn image retrieval with no human annotation," *IEEE Transactions on Pattern Analysis and Machine Intelligence*, vol. 41, no. 7, 2019.
- [38] P. Yin, A. Abuduweili, S. Zhao, L. Xu, C. Liu, and S. Scherer, "Bioslam: A bioinspired lifelong memory system for general place recognition," *IEEE Transactions on Robotics*, vol. 39, no. 6, 2023.
- [39] A. van den Oord, Y. Li, and O. Vinyals, "Representation learning with contrastive predictive coding," 2019.
- [40] F. Schroff, D. Kalenichenko, and J. Philbin, "Facenet: A unified embedding for face recognition and clustering," in *IEEE Conference on Computer Vision and Pattern Recognition*, 2015.
- [41] A. Hermans, L. Beyrer, and B. Leibe, "In defense of the triplet loss for person re-identification," 2017.
- [42] K. Simonyan and A. Zisserman, "Very deep convolutional networks for large-scale image recognition," in *International Conference on Learning Representations*, 2015.
- [43] W. Maddern, G. Pascoe, C. Linegar, and P. Newman, "1 year, 1000 km: The oxford robotcar dataset," *The International Journal of Robotics Research*, vol. 36, no. 1, 2017.
- [44] D. Olid, J. M. Fàcil, and J. Civera, "Single-view place recognition under seasonal changes," 2018.
- [45] W. Wang, D. Zhu, X. Wang, Y. Hu, Y. Qiu, C. Wang, Y. Hu, A. Kapoor, and S. Scherer, "Tartanair: A dataset to push the limits of visual slam," in *IEEE/RSJ International Conference on Intelligent Robots and Systems*, 2020.